AFRL-RX-TY-TR-2011-0096-01

# DETECTING MOTION FROM A MOVING PLATFORM;
# PHASE 1: BIOMIMETIC VISION SENSOR

John E. McInroy
Cameron H.G. Wright
Steven F. Barrett
John F. O'Brien
Farhad Jafari

University of Wyoming
1000 East University Avenue
Laramie, WY 82072

Contract No. FA4819-07-C-0010

November 2011



## AIR FORCE RESEARCH LABORATORY
## MATERIALS AND MANUFACTURING DIRECTORATE

■ **Air Force Materiel Command** ■ **United States Air Force** ■ **Tyndall Air Force Base, FL 32403-5323**

# DISCLAIMER

# NOTICE AND SIGNATURE PAGE

Using Government drawings, specifications, or other data included in this document for any purpose other than Government procurement does not in any way obligate the U.S. Government. The fact that the Government formulated or supplied the drawings, specifications, or other data does not license the holder or any other person or corporation; or convey any rights or permission to manufacture, use, or sell any patented invention that may relate to them.

This report was cleared for public release by the 88th Air Base Wing Public Affairs Office at Wright Patterson Air Force Base, Ohio available to the general public, including foreign nationals. Copies may be obtained from the Defense Technical Information Center (DTIC) (http://www.dtic.mil).

AFRL-RX-TY-TR-2011-0096-01 HAS BEEN REVIEWED AND IS APPROVED FOR PUBLICATION IN ACCORDANCE WITH ASSIGNED DISTRIBUTION STATEMENT.

WIT.JEFFREY.S.1256405292 Digitally signed by WIT.JEFFREY.S.1256405292 DN: c=US, o=U.S. Government, ou=DoD, ou=PKI, ou=USAF, cn=WIT.JEFFREY.S.1256405292 Date: 2012.02.22 15:34:11 -06'00'

JEFFREY S. WIT, PhD
Work Unit Manager

SKIBBA.BRIAN.K.1263420981 Digitally signed by SKIBBA.BRIAN.K.1263420981 DN: c=US, o=U.S. Government, ou=DoD, ou=PKI, ou=USAF, cn=SKIBBA.BRIAN.K.1263420981 Date: 2012.03.05 08:21:01 -06'00'

BRIAN K. SKIBBA, DR-III
Acting Chief, Airbase Engineering Development Branch

RHODES.ALBERT.N.III.1175488622 Digitally signed by RHODES.ALBERT.N.III.1175488622 DN: c=US, o=U.S. Government, ou=DoD, ou=PKI, ou=USAF, cn=RHODES.ALBERT.N.III.1175488622 Date: 2012.03.29 12:03:50 -05'00'

ALBERT N. RHODES, PhD
Chief, Airbase Technologies Division

**REPORT DOCUMENTATION PAGE**

*Form Approved*
*OMB No. 0704-0188*



**1. REPORT DATE** *(DD-MM-YYYY)*
30-NOV-2011

**2. REPORT TYPE**
Final Technical Report

**3. DATES COVERED** *(From - To)*
03-SEP-2007 -- 02-NOV-2011

**4. TITLE AND SUBTITLE**
Detecting Motion from a Moving Platform;
Phase 1: Biomimetic Vision Sensor

**5a. CONTRACT NUMBER**
FA4819-07-C-0010

**5b. GRANT NUMBER**

**5c. PROGRAM ELEMENT NUMBER**
0909999F

**5d. PROJECT NUMBER**
GOVT

**5e. TASK NUMBER**
F0

**5f. WORK UNIT NUMBER**
QF503003

**6. AUTHOR(S)**
McInroy, John E.; Wright, Cameron H.G.; Barrett, Steven F.;
O'Brien, John F.; Jafari, Farhad

**7. PERFORMING ORGANIZATION NAME(S) AND ADDRESS(ES)**
University of Wyoming
1000 East University Avenue
Laramie, WY 82072

**8. PERFORMING ORGANIZATION REPORT NUMBER**

**9. SPONSORING/MONITORING AGENCY NAME(S) AND ADDRESS(ES)**
Air Force Research Laboratory
Materials and Manufacturing Directorate
Airbase Technologies Division
139 Barnes Drive, Suite 2
Tyndall Air Force Base, FL 32403-5323

**10. SPONSOR/MONITOR'S ACRONYM(S)**
AFRL/RXQES

**11. SPONSOR/MONITOR'S REPORT NUMBER(S)**
AFRL-RX-TY-TR-2011-0096-01

**12. DISTRIBUTION/AVAILABILITY STATEMENT**

Distribution Statement A: Approved for public release; distribution unlimited.

**13. SUPPLEMENTARY NOTES**

Ref Public Affairs Case # 88ABW-2012-2026, 5 April 2012. Document contains color images.

**14. ABSTRACT**

The University of Wyoming has formed a robotics initiative consisting of three distinct parts.
"**Biomimetic Vision Sensor**," (AFRL-RX-TY-TR-2011-0096-01) develops a novel computer vision sensor based upon the biological vision system of the common housefly, *Musca domestica*.
"**Lightweight, Low Power Robust Means of Removing Image Jitter,**" (AFRL-RX-TY-TR-2011-0096-02) develops an optimal platform stabilization mechanism for motion detection and target tracking using recent advances in the area of Parallel Kinematic Machines (PKMs).
"**Unification of Control and Sensing for More Advanced Situational Awareness,**" (AFRL-RX-TY-TR-2011-0096-03) develops a multi-purpose planning scheme that effectively solves patrolling and constrained sensor planning problems for a large-scale multi-agent system.

**15. SUBJECT TERMS**

vibration isolation; precise pointing; robotic patrolling

| 16. SECURITY CLASSIFICATION OF: a. REPORT | b. ABSTRACT | c. THIS PAGE | 17. LIMITATION OF ABSTRACT | 18. NUMBER OF PAGES | 19a. NAME OF RESPONSIBLE PERSON |
|---|---|---|---|---|---|
| U | U | U | UU | 28 | Jeffrey S. Wit |
| | | | | | 19b. TELEPHONE NUMBER *(Include area code)* |

Reset

**Standard Form 298** (Rev. 8/98)
Prescribed by ANSI Std. Z39.18

**TABLE OF CONTENTS**

LIST OF FIGURES .......... ii
1. EXECUTIVE SUMMARY .......... 1
2. INTRODUCTION .......... 2
3. METHODS, ASSUMPTIONS, AND PROCEDURES .......... 5
4. RESULTS AND DISCUSSION .......... 7
4.1. Sensor Designs .......... 7
4.2. Modeling and Simulation .......... 8
4.3. Hardware Verification and Testing .......... 14
4.4. Light Adaptation .......... 15
4.5. Edge Detection and Orientation .......... 19
4.6. Scholarly Outputs from this Project .......... 20
5. CONCLUSIONS .......... 22
6. REFERENCES .......... 23
LIST OF SYMBOLS, ABBREVIATIONS, AND ACRONYMS .......... 26

## LIST OF FIGURES

**Page**

Figure 1. Scanning Electron Microscope Image of *Musca domestica*, with a Depiction of the Associated First Layer Neural "Wiring" Superimposed that Shows Neural Superposition ....................3
Figure 2. Depiction of Overlapping Gaussian Response Similar to that Exhibited by the Compound Eye of the Common House Fly, *Musca domestica* ....................3
Figure 3. Simplified Diagram Showing Gaussian Overlapping Photoreceptor Response and Neural Superposition; Each Hexagonal Structure in (a) is Called an Ommatidium....................4
Figure 4. Optical Front-end of a Sensor Prototype using a Planar Surface for All the Photodetectors; This Prototype Includes 49 Optical Axes ....................7
Figure 5. Optical Front-end of a Sensor Prototype using a Non-planar Angled Surface; This Prototype is Intended to be used with 49 Optical Axes ....................7
Figure 6. Size Comparison of Optical front-ends: (left) First Generation, for a Maximum of Seven Optical Channels, Built as Part of the Previous Contract; (middle) Optical Front-end of the 49-axis Sensor shown in Figure 4; (right) Alternative Optical Front-end using Optical Fibers and a Truly Curved Surface ....................8
Figure 7. Output from Large Scale Computer Simulation of Fly Eye Vision System Showing Extraction of Object Velocity Vector Information ....................9
Figure 8. Extraction of Velocity Vector Information for Line Objects ....................10
Figure 9. Extraction of Velocity Vector Information for Point Objects ....................11
Figure 10. Extraction of Flow Field Information; Simulation Shows the Platform on Which the Sensor is Mounted Moving Toward a Rectangular Object or Opening....................12
Figure 11. GUI for Changing Many Parameters of Fly Eye Sensor Simulations....................13
Figure 12. GUI for displaying Simulation Results; Buttons at the Top of the Display Window become Active when an Image is Displayed ....................13
Figure 13. Two Methods of Positioning Optical Axes for Photodetectors for the Fly Eye Sensor: (left) Hexagonal Pattern; (right) "Natural" Pattern....................14
Figure 14. Test Results Showing Desired Gaussian Overlap in Sensor Array Prototypes: ILA: Indoors, with Light Adaptation; OLA: Outdoors, with Light Adaptation; PdA: Photodiode Prototype, as in Figure 4; OFA: Optical Fiber Prototype, as in Figure 6 (right) ....................15
Figure 15. Light Adaptation Circuit Implementing a "Log Transform-Subtraction-Multiplication" Process....................16
Figure 16. Absolute Value Circuit used in the Time Delay Subsystem; This Operation is Sometimes Referred to as "Precision Rectification" ....................17
Figure 17. Time Delay Subsystem used in Conjunction with the Light Adaptation Circuitry......18
Figure 18. Horizontal Edge Localization, Indoor Environment ....................19
Figure 19. Horizontal Edge Localization, Outdoor Environment....................20

# 1. EXECUTIVE SUMMARY

The University of Wyoming has formed a robotics initiative consisting of three distinct parts. A complete, stand-alone final technical report is presented for each phase. Phase 1 was managed by Dr. Cameron Wright, Phase 2 by Dr. John O'Brien, and Phase 3 by Dr. John McInroy. The overall project was coordinated by the Robotics Initiative Manager, Dr. John McInroy.

Phase 1, "**Biomimetic Vision Sensor**," AFRL-RX-TY-TR-2011-0096 summarizes the development of a novel computer vision sensor based upon the biological vision system of the common housefly, *Musca domestica*. Several variations of this sensor were designed, simulated extensively, and hardware prototypes were constructed and tested. Initial results indicate much greater sensitivity to object motion than traditional sensors, and the promise of very high speed extraction of key image features. The main contributions of this research include: (1) characterization of the image information content presented by a biomimetic vision sensor, (2) creation of algorithms to extract pertinent image features such as object edges from the sensor data, (3) fabrication and characterization of sensor prototypes, (4) creation of an automated sensor calibration subsystem, (5) creation of a light adaptation subsystem to permit use of the sensor in both indoor and outdoor real-world environments.

The pages that follow constitute a complete, stand-alone final technical report for Phase 1.

## 2. INTRODUCTION

AFRL has identified a need for more capable vision sensors than the traditional charge coupled device (CCD) or complementary metal oxide semiconductor (CMOS) arrays. In particular, there is a need for a low-cost, inexpensive sensor that exhibits fast data throughput, is extremely sensitive to even tiny object movements, is relatively unaffected by changes in ambient light levels, and can extract pertinent image information without the need for high-end and power hungry computer central processing units (CPU). The biomimetic vision sensor described in this report is being developed to provide these capabilities. Applications for such a sensor would include remotely controlled unmanned ground or air vehicles, perimeter security, and autonomous or semi-autonomous mobile robots.

Both CCD and CMOS focal-plane array sensors are commonly used and perform well in many imaging applications, but have certain drawbacks for applications that require high sensitivity to motion and high speed extraction of certain image features such as object edges [1-5]. For example, when using standard CCD or CMOS sensors, objects moving at high speed appear blurred and have low contrast, objects moving less than a pixel across the array appear not to have moved at all, and if edge information is needed it requires significant computation of a computer's CPU.

To create a vision sensor that overcomes these drawbacks, a biomimetic (also known as "biologically inspired") engineering approach was embraced to take advantage of proven biological "designs" found in the animal kingdom and then adapt salient aspects of these into more capable designs. This biomimetic vision sensor is based on physiological aspects of the eye (and vision-related neural layers) of the common housefly, *Musca domestica*. The fly has a tiny brain, yet exhibits visual feats that exceed the best traditional computer vision systems. This implies that a biomimetic vision sensor design that is based on the compound eye of the housefly could eliminate the need for a high performance computer CPU (the "brain") in the vision system, and allow greater capability on certain vision tasks (such as motion detection) than is possible with traditional sensors. The fly eye has been extensively studied over many years, and the research presented here has leveraged this large body of knowledge in the development of a biomimetic vision sensor [6-30].

Such a biomimetic "fly eye" vision sensor would be extremely sensitive to object motion, even tiny motions that standard imaging sensors would miss entirely (called "motion hyperacuity" in the literature [10]), and be able to extract key object features such as edges at very high speed with no CPU involvement. The fly exhibits these traits, so a properly designed biomimetic vision sensor based on the fly should also exhibit these traits.

The fly uses a combination of quasi-Gaussian overlapping photoreceptor responses and neural superposition to achieve what has been described in the literature as "hyperacuity," or the ability to detect image features, such as object motion, to a much higher degree than just the photoreceptor density would imply. See Figure 1 for an image of the fly eye, and Figure 2 for an image of overlapping Gaussian responses.

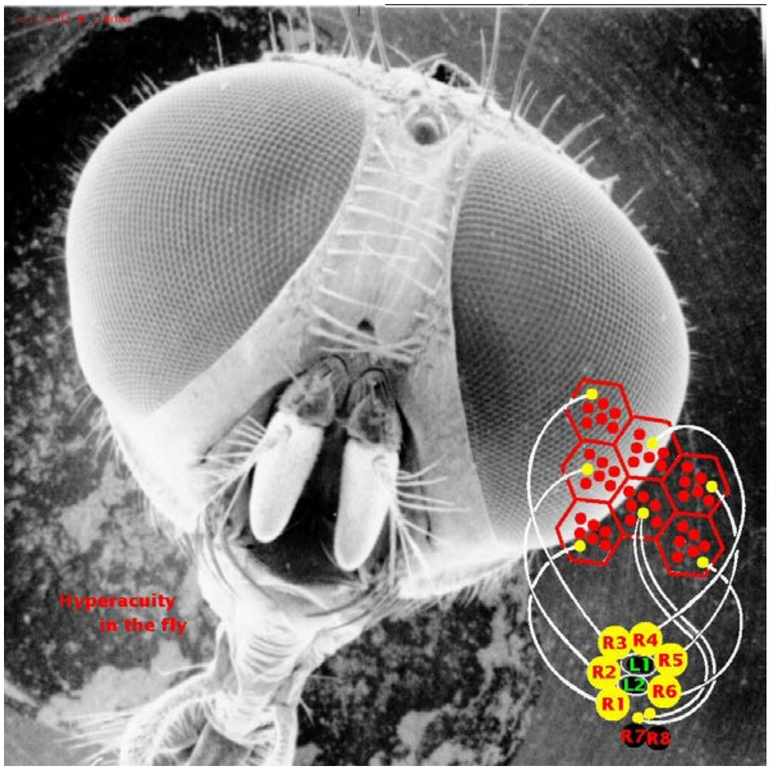


**Figure 1. Scanning Electron Microscope Image of *Musca domestica*, with a Depiction of the Associated First Layer Neural "Wiring" Superimposed that Shows Neural Superposition**

*Image courtesy of M. Wilcox.*

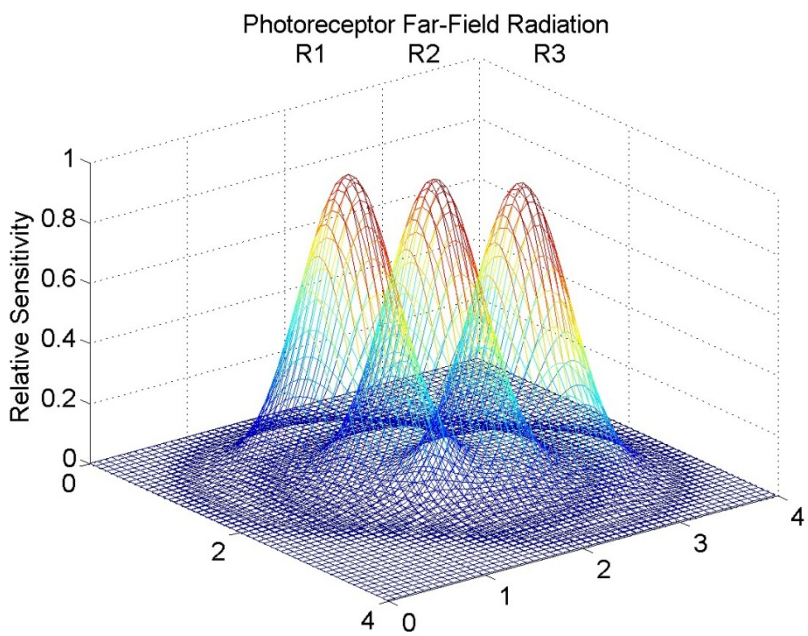


**Figure 2. Depiction of Overlapping Gaussian Response Similar to that Exhibited by the Compound Eye of the Common House Fly, *Musca domestica***

Figure 3 shows a simplified diagram to illustrate this quasi-Gaussian (henceforth called simply "Gaussian") overlapping photoreceptor response and neural superposition that both contribute to such desirable sensor capabilities. In this figure, the seven shaded photoreceptors from seven physically distributed ommatidia (the structural elements that make up an insect's compound eye) shown in (a) all view the same point at infinity. The overlapping visual field of the three receptors depicted in (b) is shown as (c). All seven visual fields (as half power radii) are shown perpendicular to the optical axis in (d). Signals from the physically distributed but optically co-aligned photoreceptors combine in the neural layer and together are called a "cartridge." While the fly has eight photoreceptors in each ommatidium, (Figure 1), receptors R7 and R8 are "stacked" and share a single optical axis. Note that the Gaussian overlap for an artificial sensor comes from the front-end optical design, whereas the neural superposition is accomplished by how the signals are subsequently combined.

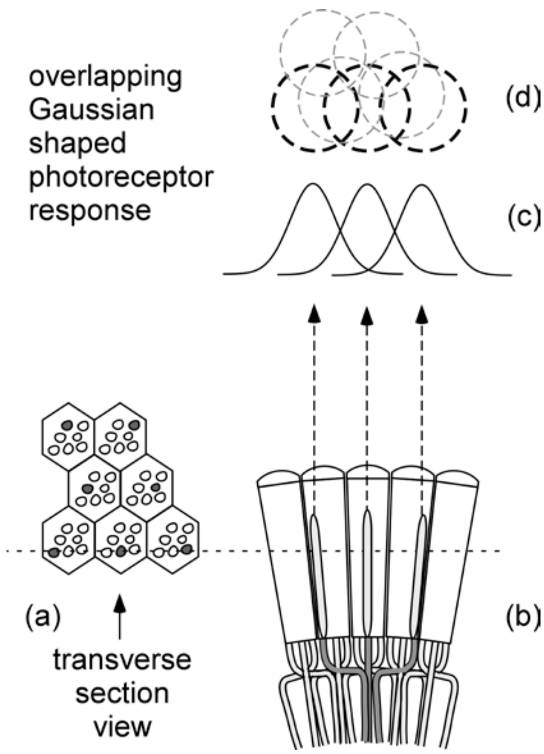


**Figure 3. Simplified Diagram Showing Gaussian Overlapping Photoreceptor Response and Neural Superposition; Each Hexagonal Structure in (a) is Called an Ommatidium**

The research challenges of this effort were to better understand how the fly eye achieved capabilities such as motion hyperacuity; to create an optically valid but low-cost and easily manufactured design approach that mimicked the salient aspects of the fly eye; and to develop algorithms that could process the signals from such a sensor in order to extract desired image information such as object motion or object edges.

## 3. METHODS, ASSUMPTIONS, AND PROCEDURES

The methodology for building the fly eye sensor was performed in a building block approach. The research described in this report is a continuation of an earlier project that was performed under Contract No. FA4819-07-C-0003. This earlier work explored the physiological aspects of the fly eye that were pertinent to the desired capabilities, designed the opto-electronic equivalent of a single sensor element similar in many ways to one photoreceptor in a single ommatidium of the compound eye of the fly (exhibiting the characteristic Gaussian response), investigated the signal content of such a sensor, created a small one-dimensional array of sensors with overlapping Gaussian visual fields, investigated the signal content of the 1D array, and devised algorithms to extract key image features such as object motion. Based upon what was learned in this earlier project, the current project proceeded to create several designs for a two-dimensional array constructed from two-dimensional versions of the individual sensor elements. Industry-standard optical design software, Zemax, was used to explore various optical configurations that led to the optical front-ends of the hardware prototypes.

Extensive simulation was performed for each sensor design to ensure the desired characteristics of motion hyperacuity and feature extraction would be exhibited. To help with the many simulations, a highly flexible simulation software framework with a graphical user interface (GUI) was created for a wide variety of sensor parameters.

Once the simulation results were satisfactory, hardware prototypes of the sensor designs were built. Three environments were used for testing the prototypes: a small, highly controllable “light box” where the ambient lighting could be adjusted easily; a large “light room” with white fabric on all walls where variations on typical indoor lighting conditions could be introduced (both fluorescent and incandescent) and where there would be sufficient room to move target objects across the sensor field of view to test for motion and edge extraction; and an outdoor area where the sensor could be exposed to much more challenging but realistic lighting scenarios found outside. Results from these tests are described in the Results and Discussion section. Additional subsystems were also designed for the sensors, including a 49-channel custom data acquisition unit, an automated sensor calibration subsystem, and a light adaptation subsystem.

Early results of the outdoor testing confirmed expectations that the dynamic range of ambient lighting from indoor to outdoor environments exceeded capability of a linear sensor interface. Due to the parallel and analog nature of the sensor, methods to adjust for ambient lighting used in traditional CCD or CMOS cameras would not work. For example, traditional focal plane array (CCD or CMOS) cameras control the amount of light incident on the array by adjusting an aperture in the single complex lens system and control the integration time of the light by adjusting a mechanical and/or electronic shutter. Since the fly eye sensor is based on a compound eye with many small simple lenses, having individual photodetectors for each of many optical axes, an aperture/shutter approach is not feasible. The fact that each of many optical axes results in many channels of electronics also constrains the use of traditional automatic gain control (AGC) electronics. The design solution to this is described in the Results and Discussion section.

One assumption made was that the sensor design could forego the physical separation of the photoreceptors that make up a biological neural cartridge (Figure 2), as long as the optical axes aligned correctly and the visual fields exhibited the proper amount of Gaussian overlap. This assumption would eliminate many manufacturing difficulties, and it was hypothesized that similar visual performance could still be obtained. Another assumption made was that all signal/image processing algorithms used with the sensor must consist only of very basic operations such as multiplication, division, addition, and subtraction since that is all that the neural interconnects in the fly eye were capable of performing, and that adhering to this would allow for the implementation of the signal processing in low-cost but very fast parallel analog hardware. These assumptions were validated during testing, as discussed in Section 4.

## 4. RESULTS AND DISCUSSION

The following summarizes some key aspects of the results. Note that this work is a follow-on to an earlier contract, so this section builds on results described in the previous report, AFRL-RX-TY-TR-2009-4518.

### 4.1. Sensor Designs

Based on work performed in the earlier contract with one-dimensional sensors, three versions of a two-dimensional sensor were designed: one mounted on a planar (flat) surface, one mounted on an angled surface that approximated the curved surface of the fly eye, and one on a truly curved surface. These prototypes are listed in increasing order of manufacturing difficulty. Figures 4–6 depict these 2D sensor prototype variations. The angled optical front-end shown in Figure 5 was an intermediate step between the flat sensor and curved sensor (middle and right of Figure 6, respectively). As such, it received the least amount of testing.

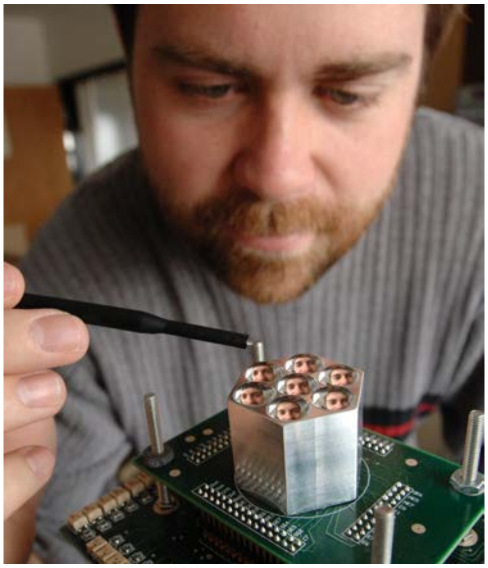

**Figure 4. Optical Front-end of a Sensor Prototype using a Planar Surface for All the Photodetectors; This Prototype Includes 49 Optical Axes**

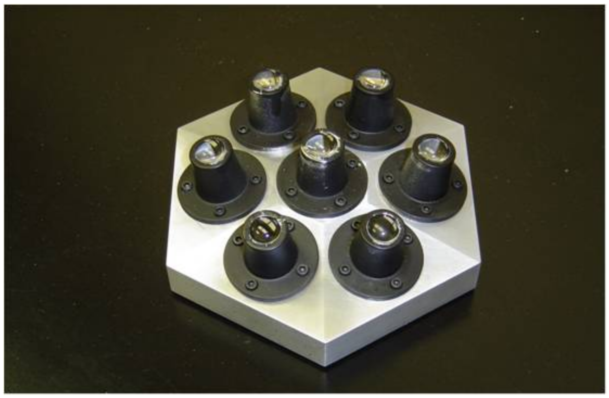

**Figure 5. Optical Front-end of a Sensor Prototype using a Non-planar Angled Surface; This Prototype is Intended to be used with 49 Optical Axes**

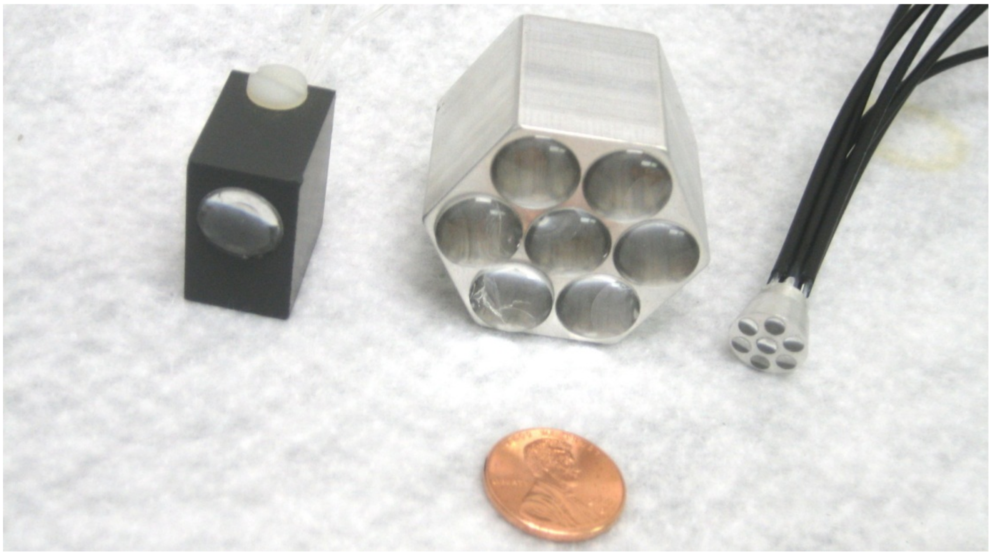

**Figure 6. Size Comparison of Optical front-ends: (left) First Generation, for a Maximum of Seven Optical Channels, Built as Part of the Previous Contract; (middle) Optical Front-end of the 49-axis Sensor shown in Figure 4; (right) Alternative Optical Front-end using Optical Fibers and a Truly Curved Surface**

## 4.2. Modeling and Simulation

Simulations were performed using both Zemax and MATLAB. In particular, the various tradeoffs for light propagation through the front-end optics were investigated by simulating with Zemax, then building the physical optics for the best configuration. The simulations related to the first neural layer processing of image features such as edges, motion vectors, and such were performed with MATLAB.

These simulations provided considerable insight into the potential capabilities of a biomimetic sensor based upon the fly eye. For instance, the ability to easily extract edge information, normally a computer-intensive process, was shown to be possible using simple operations that could be implemented in very fast parallel analog circuitry in an actual hardware sensor system, reducing CPU overhead to nearly zero. Similarly, the large-scale simulation model showed that a fly eye sensor should be able to extract velocity vector (and hence flow field) information. An example of this is shown in Figure 7, where six ping pong balls were bounced in a transparent container and the simulation provided velocity vectors for each object in such a way that there would be nearly zero CPU overhead for an actual sensor system.

The smaller, more specific computer models that more closely simulated the various sensor prototype designs confirmed these capabilities. For example, Figure 8 shows motion detection and velocity vector information. The simulated objects are three vertical lines, with two of them moving in opposite directions (line A is moving to the right fast, Line B is moving to the left at a medium speed), and one (line C) is stationary. The figure shows that the stationary object is ignored while the velocity vectors of the two moving objects are extracted correctly. Note the velocity vectors represent the entire movement from the 1st to the 24th image frame.

Figure 9 shows a similar result for simulated point objects, and Figure 10 shows the result of extracting the flow field information for a simulated object approaching the sensor. Once again, note the velocity vectors represent the entire movement from the 1st to the 24th image frame.

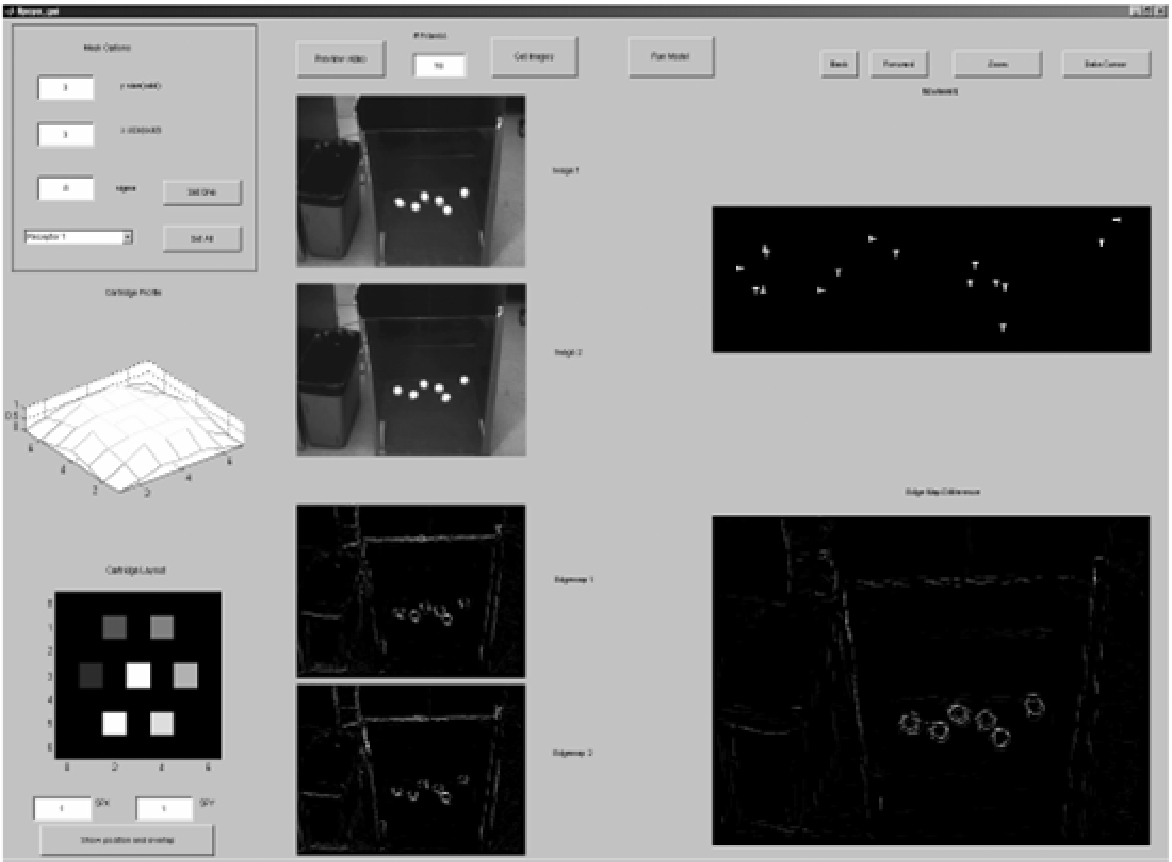

**Figure 7. Output from Large Scale Computer Simulation of Fly Eye Vision System Showing Extraction of Object Velocity Vector Information**

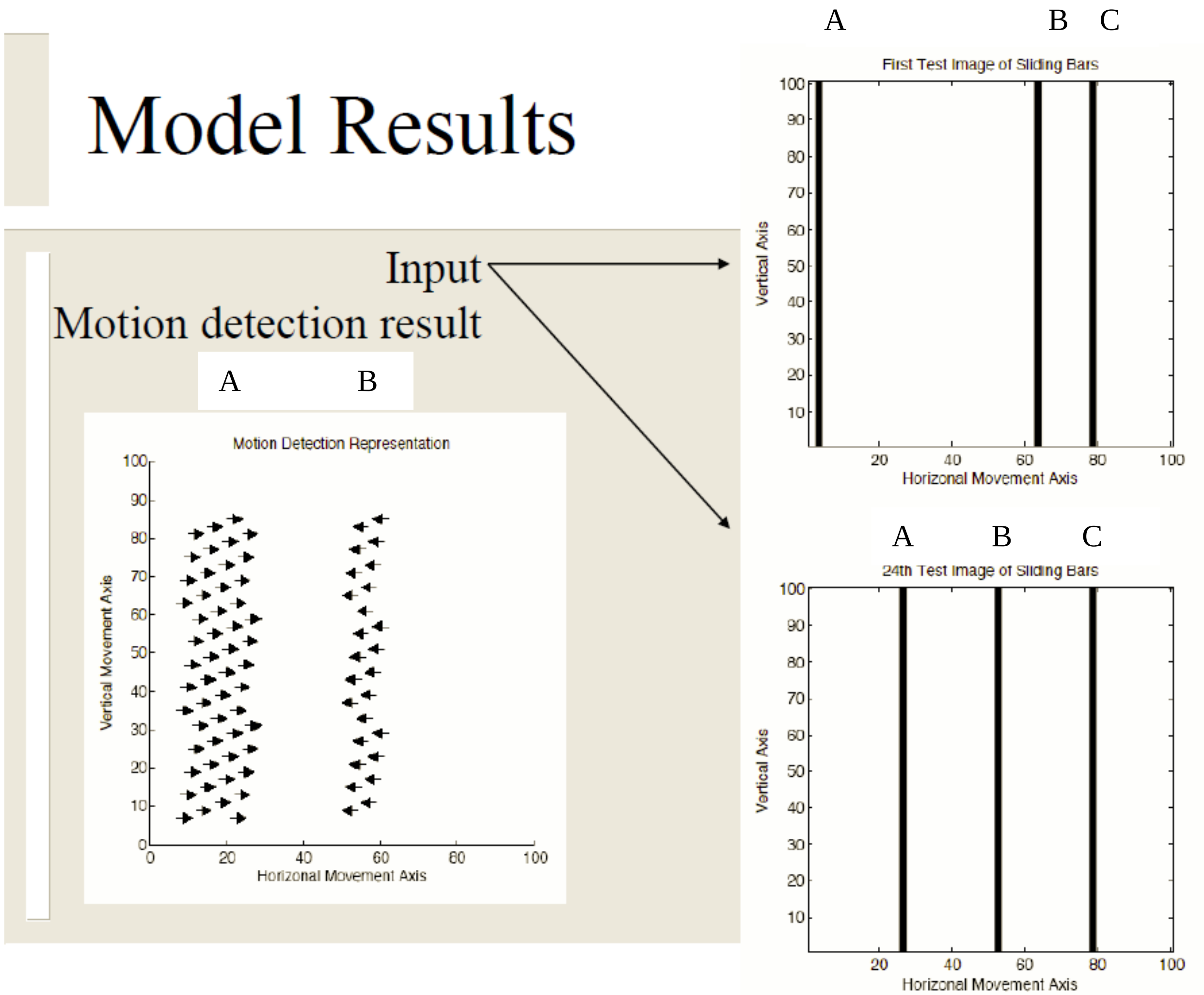


**Figure 8. Extraction of Velocity Vector Information for Line Objects**

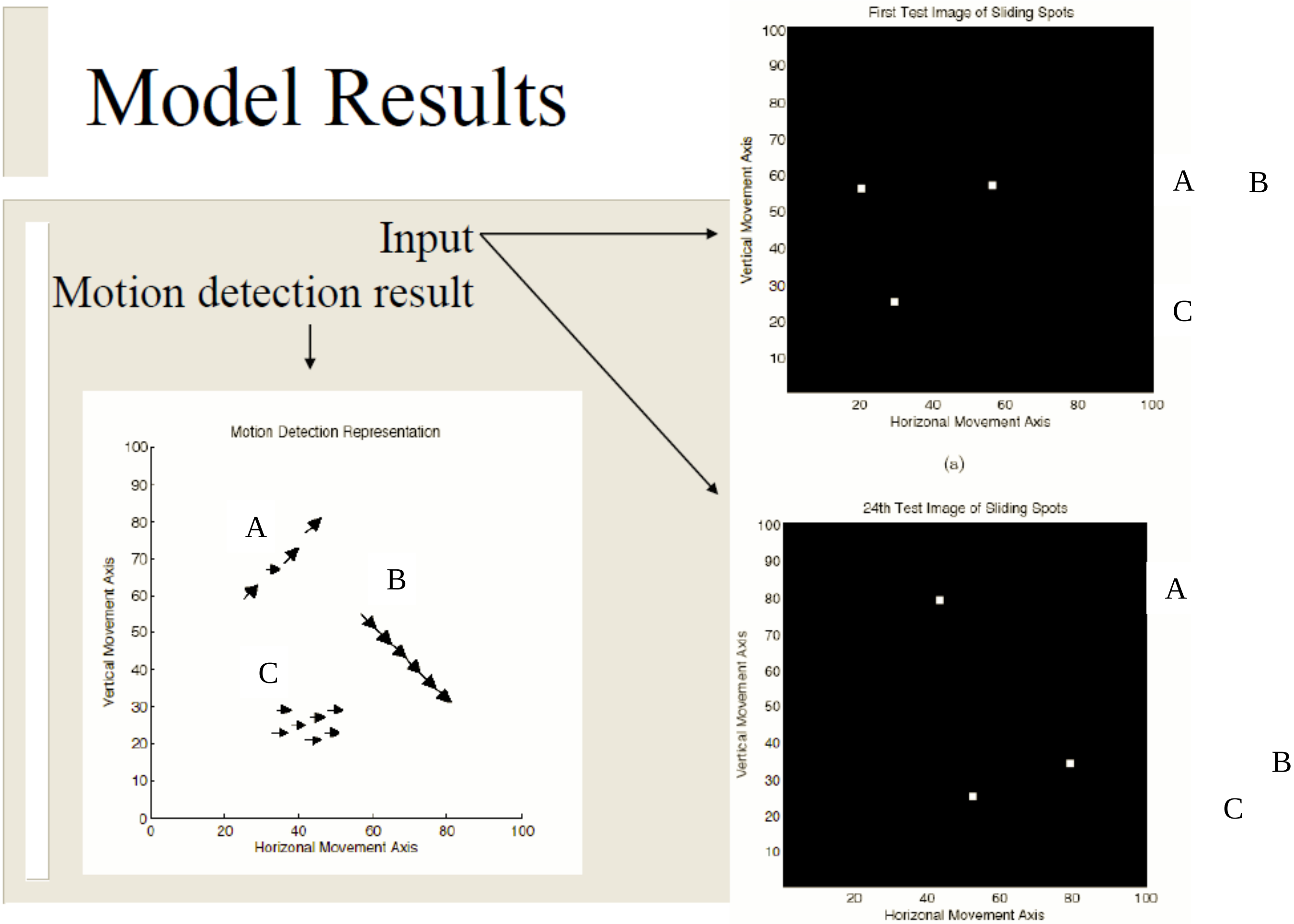


**Figure 9. Extraction of Velocity Vector Information for Point Objects**

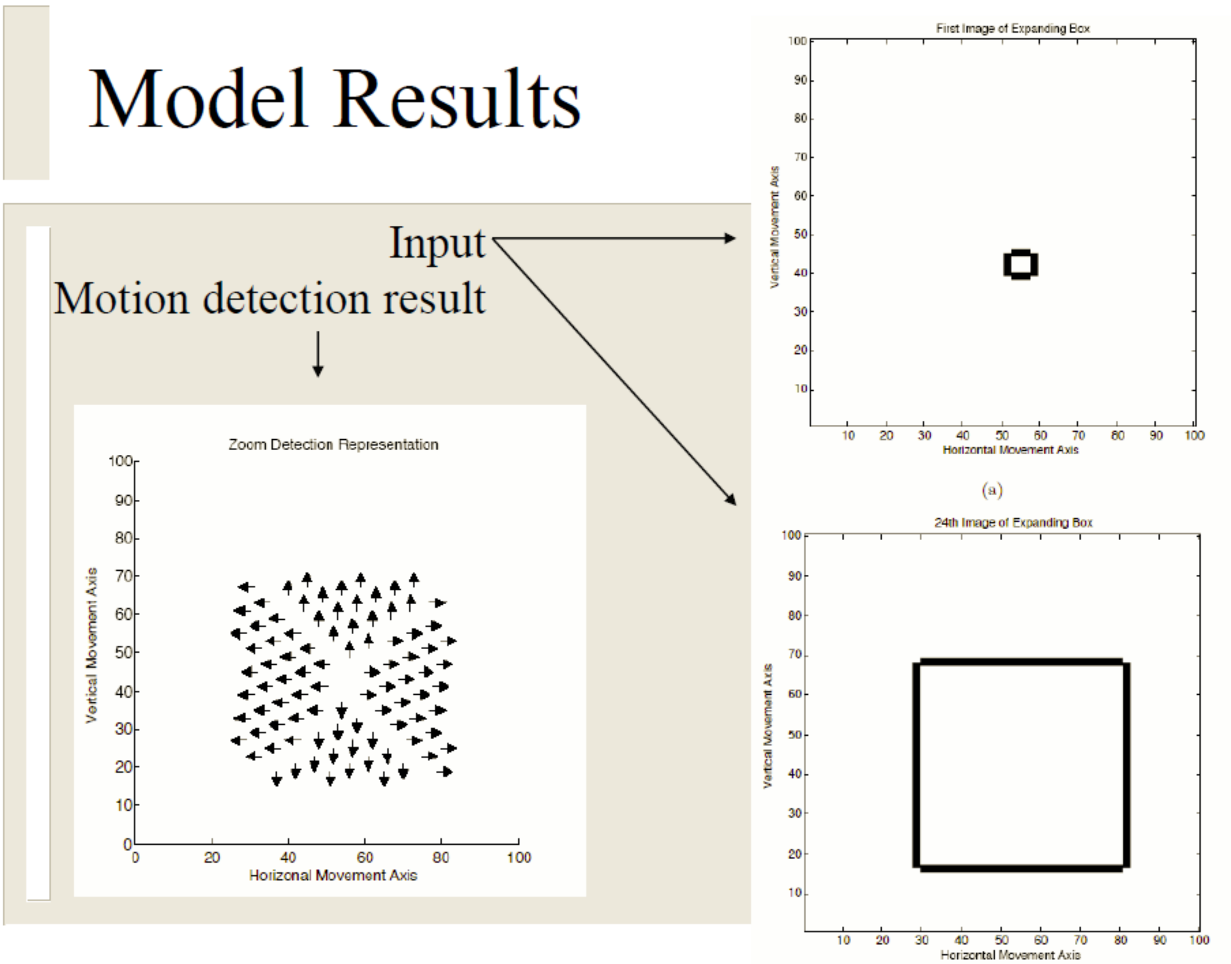


**Figure 10. Extraction of Flow Field Information; Simulation Shows the Platform on Which the Sensor is Mounted Moving Toward a Rectangular Object or Opening**

To better standardize testing and simulation of the various sensor designs, a highly flexible simulation software framework with a GUI was created that could be used to easily change a wide variety of sensor parameters. Some of the user interface elements of this software framework are shown in Figure 11 and Figure 12.

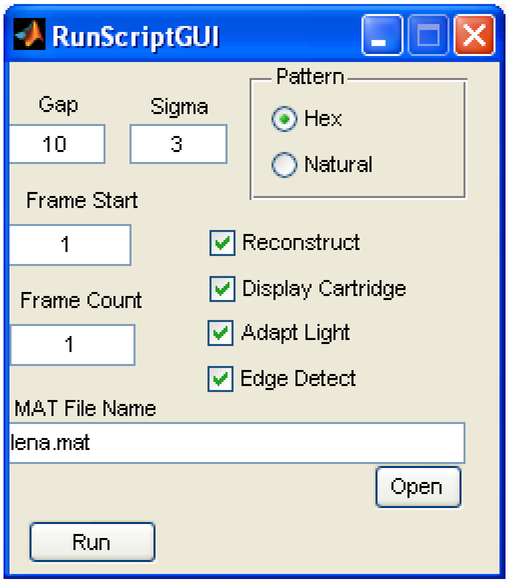


**Figure 11. GUI for Changing Many Parameters of Fly Eye Sensor Simulations**

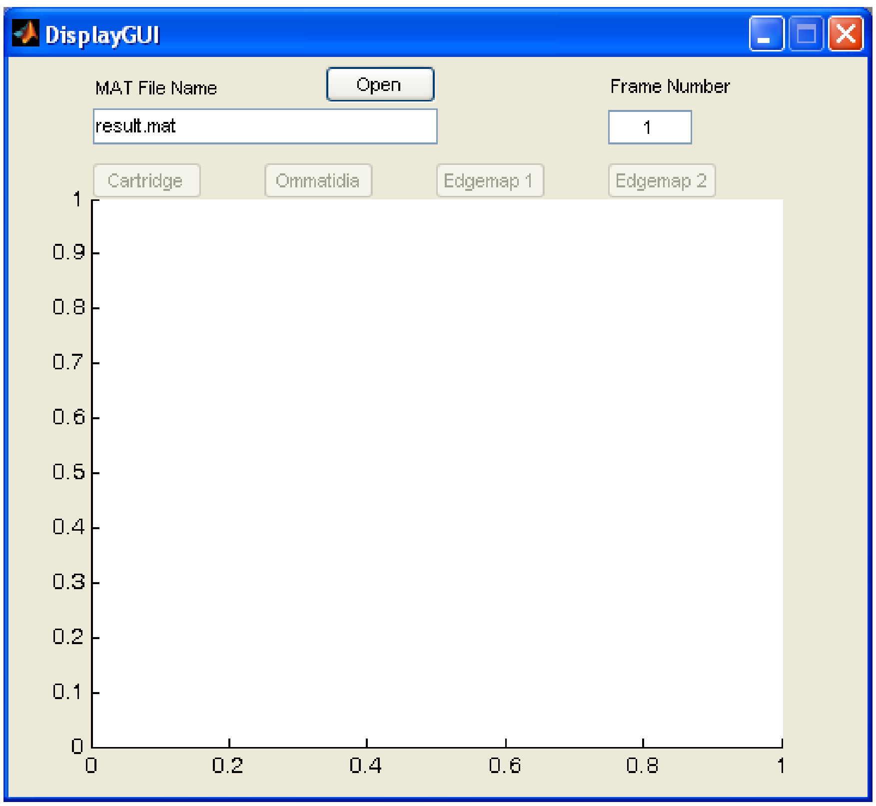


**Figure 12. GUI for displaying Simulation Results; Buttons at the Top of the Display Window become Active when an Image is Displayed**

The software framework allows the user to easily change parameters of the sensor simulation. For example, the comparison between a hexagonal pattern of photodetectors and a "natural" pattern (i.e., closer to how the fly photoreceptors occur) could be easily accomplished. These two patterns are shown in Figure 13.

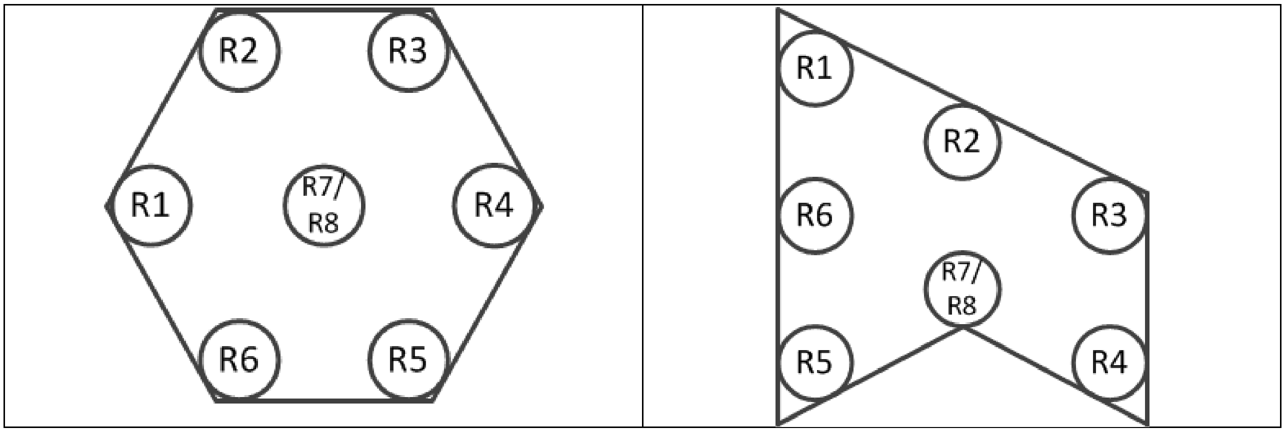


**Figure 13. Two Methods of Positioning Optical Axes for Photodetectors for the Fly Eye Sensor: (left) Hexagonal Pattern; (right) "Natural" Pattern**

## 4.3. Hardware Verification and Testing

After hardware prototypes were constructed for the biomimetic fly eye vision sensor, the electro-optical properties needed to be verified to confirm that they actually approximated the salient aspects of the fly eye. The primary aspect of interest was the overlapping Gaussian profiles. Figure 14 shows results of passing a line object past the sensor (Only three optical channels are shown); note the distinctive Gaussian shaped overlap between individual channel signals. The gain in the electronics had not been adjusted, so the heights of the Gaussians are slightly different in the figure; this was easily corrected when the gain settings were calibrated later. This figure shows many results at once: testing both indoors and outdoors, use of light adaptation described later, and two different prototype designs.

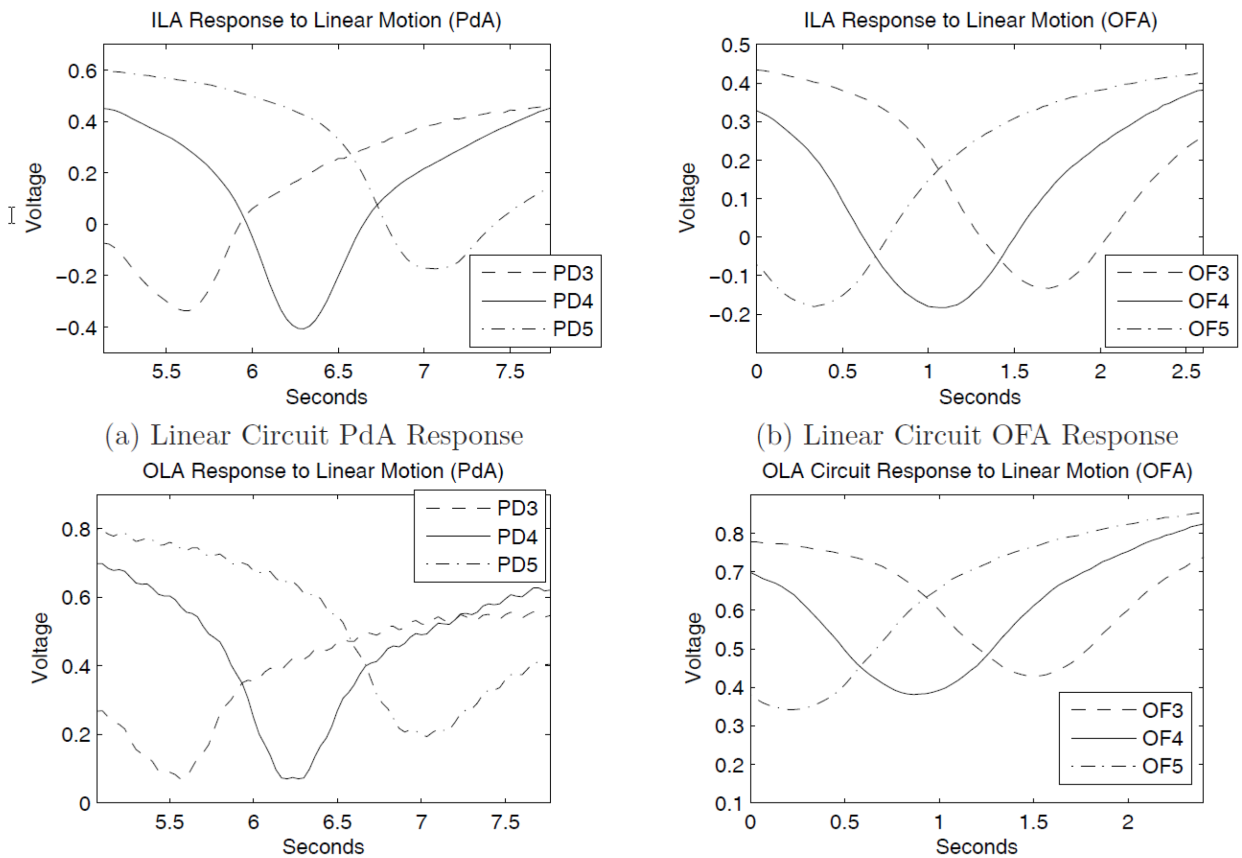


(a) Linear Circuit PdA Response
(b) Linear Circuit OFA Response
(c) Log Circuit PdA Response
(d) Log Circuit OFA Response

**Figure 14. Test Results Showing Desired Gaussian Overlap in Sensor Array Prototypes: ILA: Indoors, with Light Adaptation; OLA: Outdoors, with Light Adaptation; PdA: Photodiode Prototype, as in Figure 4; OFA: Optical Fiber Prototype, as in Figure 6 (right)**

In the previous contract, the 1D sensor array prototype was used to compare the biomimetic vision sensor to a standard CCD camera. It was investigated how well, compared to the CCD technology, the fly eye sensor could detect fast movement and also very tiny movements (i.e., translation of a very small distance). Traditional CCD sensors exhibit smearing of objects that move quickly compared to the integration time of the CCD wells, and tiny movements that do not span multiple pixels of a CCD array are undetectable to traditional sensors. Testing confirmed that the fly eye sensor was superior to the CCD camera in both aspects. It was shown in the previous report that the fly eye sensor vastly outperformed CCD arrays for responding to fast movements and tiny movements, even in very low contrast scenarios. The results for CMOS arrays would be very similar. For this report, it was verified that these same characteristics were present in the 2D fly eye sensor arrays. Additional hardware verification and testing is described in the next section on light adaptation.

## 4.4. Light Adaptation

The light adaptation subsystem had to be designed specifically for a compound eye type of sensor. As discussed in the Methods section, traditional aperture/shutter methods of controlling light are not practical for this type of sensor. The final design of the light adaptation subsystem was based biomimetically upon the “log transform-subtraction-multiplication” method observed in the biological fly. For each 7-channel optical axis grouping, this was performed using the circuit shown in Figure 15.

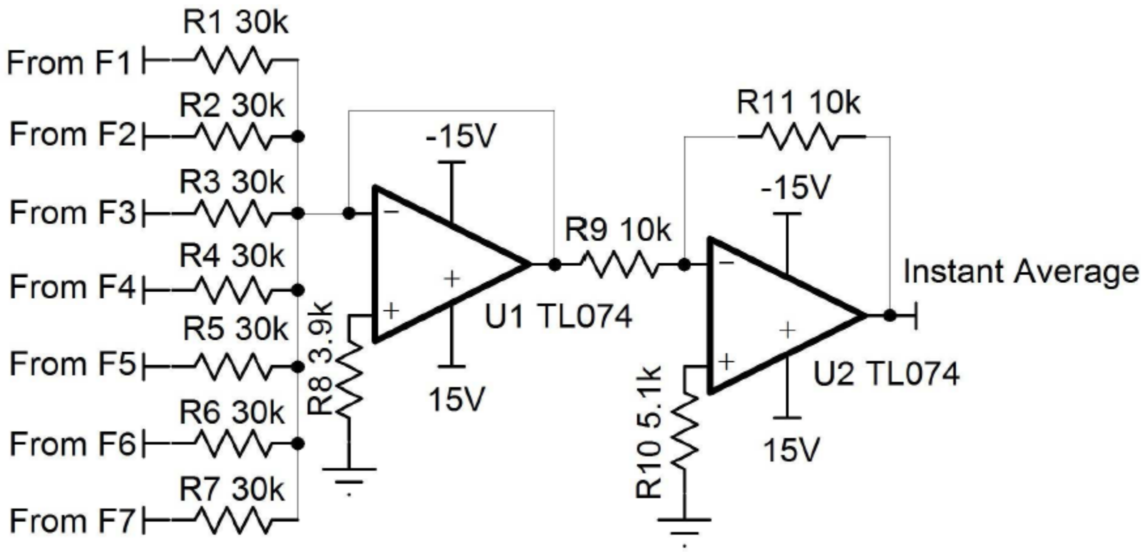


**Figure 15. Light Adaptation Circuit Implementing a “Log Transform-Subtraction-Multiplication” Process**

Used by itself, this light adaptation circuit reacts almost instantaneously, which is detrimental to the sensor performance. Light adaptation is meant to adjust for relatively slow changes in ambient lighting to allow a wider dynamic range of operation than would otherwise be possible. It was found, not unexpectedly, that if the light adaptation is allowed to be too fast, it will “adapt” to light changes due to objects of interest instead of to ambient lighting, and make objects of interest harder to detect. The solution is to add a time delay to the light adaptation subsystem. All biological creatures incorporate such a time delay into their light adaptation physiology.

Traditional electronic time delay methods, such as memory/shift registers, are not feasible due to the need to preserve the analog nature of the signal. A method such as ADC-delay-DAC would be too expensive and/or introduce too much quantization error. Older analog methods such as RC or RL delay lines suffer from poor stability and unrealistic component values for the delay needed, which was determined to be approximately one second. The resulting solution includes a sample and hold circuit with a timer that samples the analog signal, but does not quantize or digitally encode the signal. Thus delay was achieved without compromising the analog nature of the sensor signal. Circuits associated with the time delay are shown in Figure 16 and Figure 17.

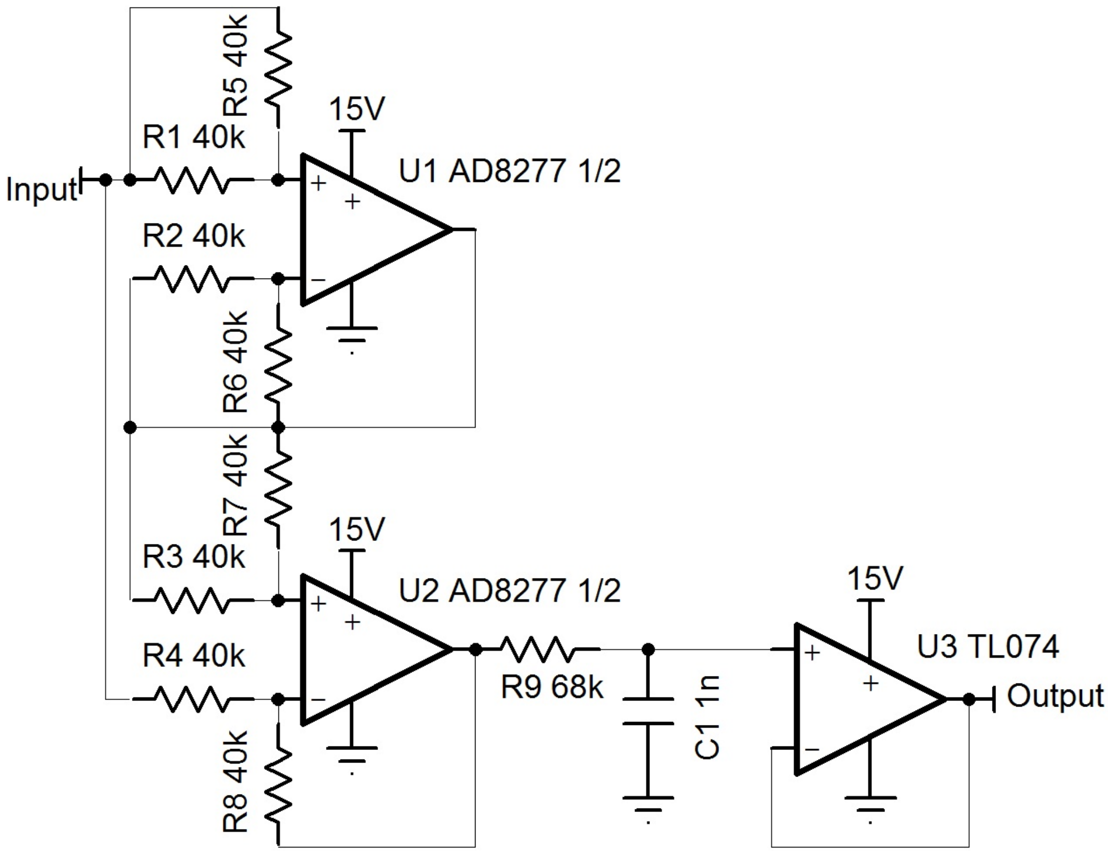


**Figure 16. Absolute Value Circuit used in the Time Delay Subsystem; This Operation is Sometimes Referred to as "Precision Rectification"**

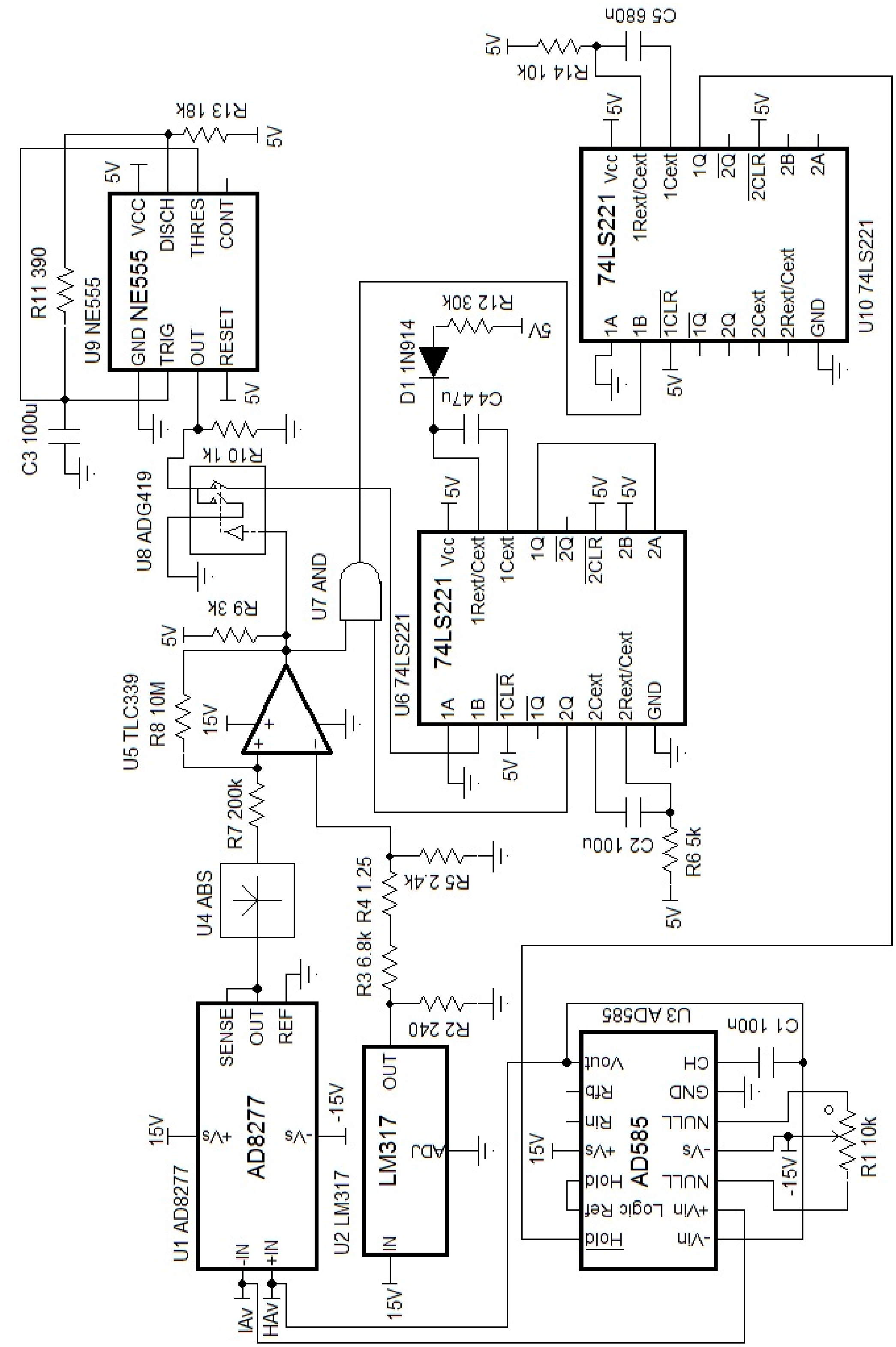

**Figure 17. Time Delay Subsystem used in Conjunction with the Light Adaptation Circuitry**

## 4.5. Edge Detection and Orientation

The sensitivity of the 2D biomimetic sensor with light adaption was already determined to have the same sensitivity to fast motion and tiny motion described in the report of the previous contract. Its ability to extract image features such as object edges and edge orientation was also tested. It is important to recall that this feature extraction is performed entirely in analog electronics, and at very high speed, with zero help from a computer. Figure 18 and Figure 19 show the sensor's ability to localize a horizontal edge of an object in its field of view for indoor and outdoor environments.

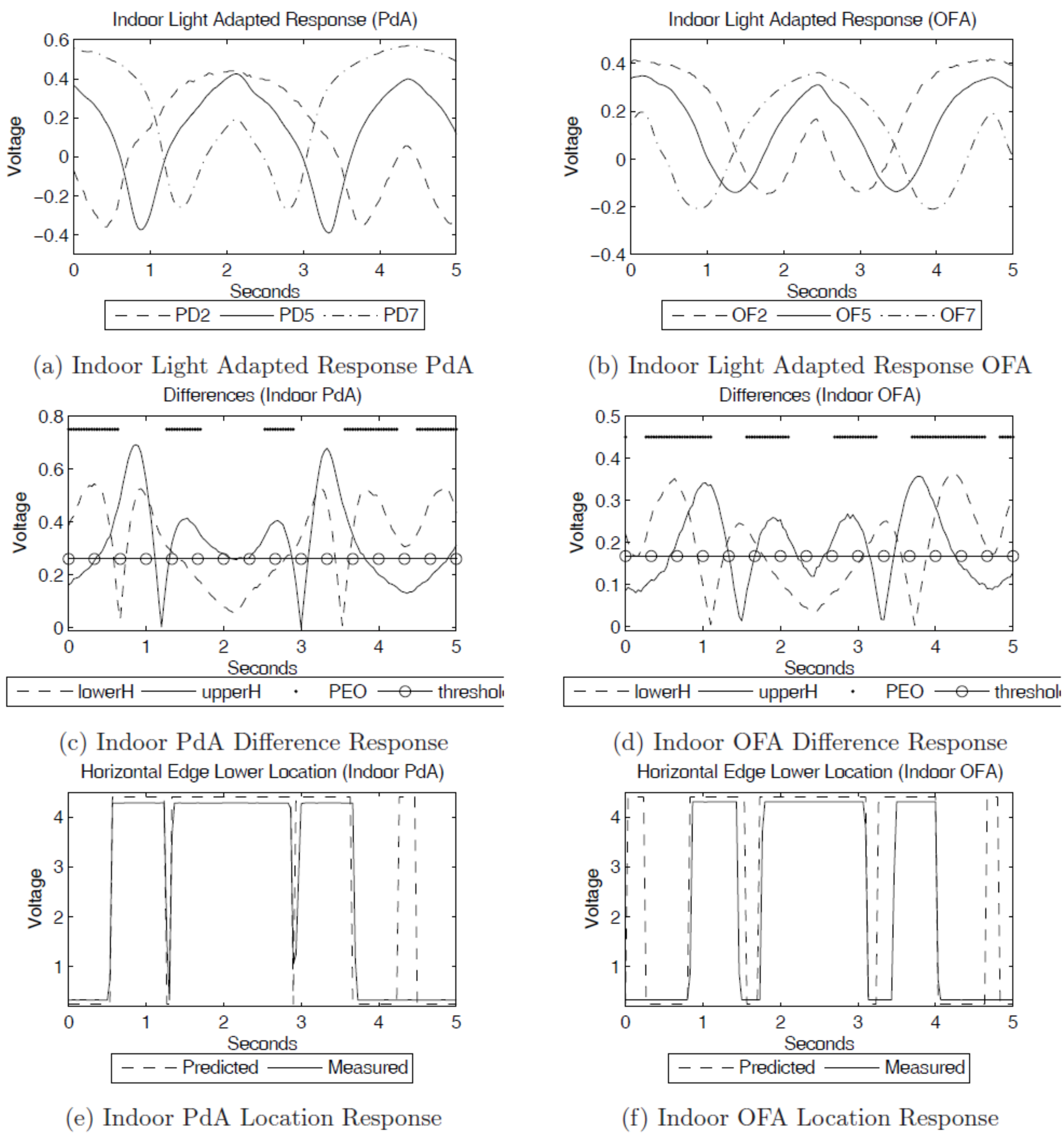


(a) Indoor Light Adapted Response PdA

(b) Indoor Light Adapted Response OFA

(c) Indoor PdA Difference Response

(d) Indoor OFA Difference Response

(e) Indoor PdA Location Response

(f) Indoor OFA Location Response

**Figure 18. Horizontal Edge Localization, Indoor Environment**

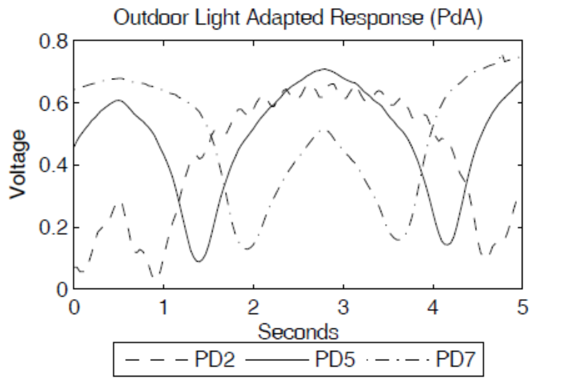


(a) Outdoor Light Adapted Response PdA

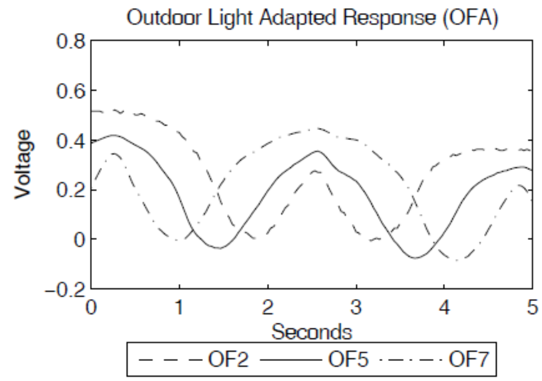


(b) Outdoor Light Adapted Response OFA

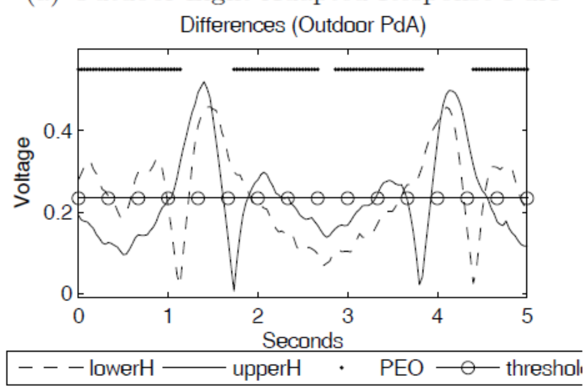


(c) Outdoor PdA Difference Response

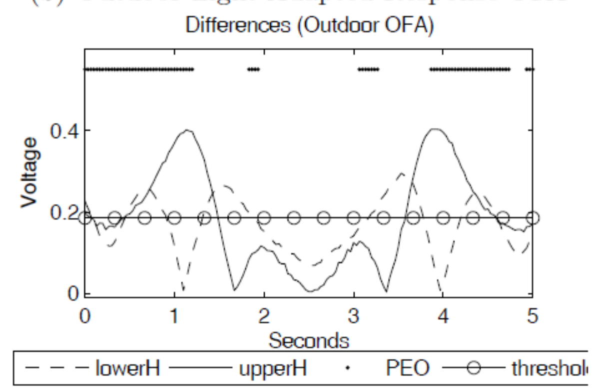


(d) Outdoor OFA Difference Response

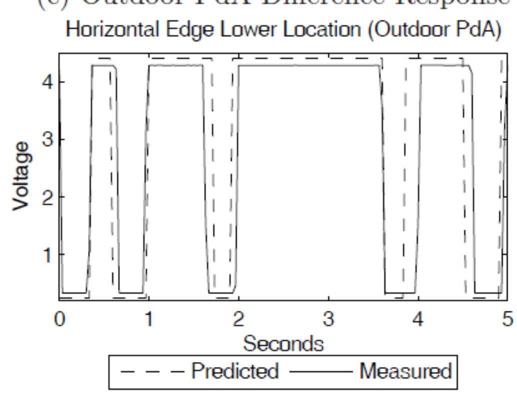


(e) Outdoor PdA Location Response

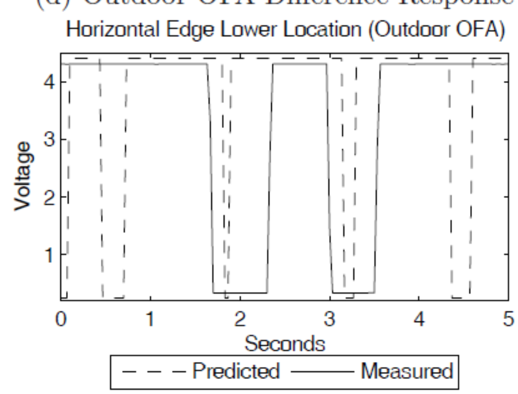


(f) Outdoor OFA Location Response

**Figure 19. Horizontal Edge Localization, Outdoor Environment**

The sensor correctly localized the majority of object horizontal edges presented to its field of view. Results for vertical and diagonal edges were very similar.

## 4.6. Scholarly Outputs from this Project

As part of this project, eight students completed M.S. degrees in Electrical Engineering (with one pending completion of requirements), and one student is in the process of completing the final requirements of the Ph.D. degree in Electrical Engineering.

A total of 16 papers describing this work were published and/or presented in journals and conferences to date [31-46]. All such papers were subjected to peer-review prior to acceptance.

## 5. CONCLUSIONS

The concept of a biomimetic fly eye vision sensor with capabilities that improve upon traditional vision sensors was validated through the work performed on this contract. The most pertinent conclusions that can be drawn from this research are discussed below.

A vision sensor based upon the fly eye shows the ability to detect object movement to a far greater degree than traditional vision sensors such as CCD (or CMOS) arrays. Fast moving objects exhibit far less smearing (and its associated loss of contrast) when using a fly eye sensor. Very slight relative object movements are also readily detected by the fly eye sensor, whereas traditional sensors require movement that spans multiple pixels before any such movement is detectable. This is termed “motion hyperacuity.” The fly eye sensor requires no special CPU processing, and does not require multiple image frames (as do many “sub-pixel” and “hyper-resolution” algorithms intended for traditional image sensors).

Detailed simulations, confirmed with hardware prototypes, show that with the fly eye sensor, important image information such as object edges, velocity vectors, and flow field information can be extracted prior to any CPU processing via fast, low-cost, parallel analog electronics. This has multiple benefits, such as lower CPU overhead, and potential reduction in image data bandwidth. All hardware test results shown in this report were obtained using only high speed analog circuitry; zero assistance from a computer was needed.

It should be noted that from an optical point of view, the overlapping Gaussian responses which help provide capabilities such as motion hyperacuity are not without some drawbacks. In particular, the incoming image is “pre-blurred” to a certain degree in order to achieve the overlapping effect. Thus traditional measures of static acuity, such as the ability to resolve line pairs in a test target image, would be lower using the fly eye sensor. The ramification of that issue is application dependent, but the general conclusion is that the fly eye sensor would probably be most valuable as one part of a hybrid vision system. As part of the hybrid system, the traditional sensor could provide higher static acuity and the fly eye sensor could provide extreme sensitivity to object movements, and high speed extraction of edges, and flow fields.

The potential of the fly eye sensor to provide vision capabilities that are far greater than traditional sensors can provide invites many exciting application scenarios that include remotely controlled unmanned ground or air vehicles, perimeter security, and autonomous or semi-autonomous mobile robots. This research has reached the threshold of significant breakthroughs in sensor technology; further development would pay great dividends.

# 6. REFERENCES


[1] J. Nakamura, *Image Sensors and Signal Processing for Digital Still Cameras*. CRC Press, 2006.

[2] G. C. Holst, *CCD Arrays, Cameras, and Displays*. SPIE Press, 1996.

[3] W. S. Boyle and G. E. Smith, “Charge coupled semiconductor devices,”*Bell Syst. Tech. J.*, vol. 49, pp. 587–593, 1970.

[4] G. C. Holst, *Electro-Optical Imaging System Performance*, 3rd ed. SPIE Press, 2003.

[5] R. H. Vollmerhausen, D. A. Reago, Jr., and R. G. Driggers, *Analysis and Evaluation of Sampled Imaging Systems*. SPIE Press, 2010.

[6] M. F. Land and D. Nilsson, *Animal Eyes*. Oxford University Press, 2002 (corrected reprint 2006).

[7] B. G. Burton and S. B. Laughlin, “Neural images of pursuit targets in the photoreceptor arrays of male and female houseflies *Musca domestica*,” *J. Exp. Biology*, vol. 206, pp. 3963–3977, 2003.

[8] M. J. Korenberg, M. Juusola, and A. S. French, “Two methods for calculating the responses of photoreceptors to moving objects,” *BMES Annals of Biomedical Engineering*, vol. 26, no. 2, pp. 308–314, Mar. 1998.

[9] M. Juusola and A. S. French, “Visual acuity for moving objects in first and second-order neurons of the fly compound eye,” *J. Neurophysiol.*, vol. 77, pp. 1487–1495, 1997.

[10] K. Nakayama, “Biological image motion processing: A review,” *Vision Research*, vol. 25, pp. 625–660, 1985.

[11] M. J. Wilcox and D. C. Thelen, Jr., “A retina with parallel input and pulsed output, extracting high-resolution information,” *IEEE Trans. Neural Net.*, vol. 10, no. 3, pp. 574–583, May 1999.

[12] T. R. Neumann, “Modeling insect compound eyes: Space-variant spherical vision,” in *Proceedings of the 2nd International Workshop on Biologically Motivated Computer Vision (BMCV 2002)*, H. H. Bulthoff, S.-W. Lee, T. A. Poggio, and C. Wallraven, Eds. Springer-Verlag, 2002, pp. 360–367.

[13] L. P. Lee and R. Szema, “Inspirations from biological optics foradvanced photonic systems,” *Science*, vol. 310, pp. 1148–1150, Nov. 2005.

[14] K.-H. Jeong, J. Kim, and L. P. Lee, “Biologically inspired artificial compound eyes,” *Science*, vol. 312, pp. 557–561, Apr. 2006.

[15] W. Snyder, “Physics of vision in compound eyes,” in *Handbook of Sensory Physiology*, H. Autrum, Ed. Springer-Verlag, 1979, vol. VII/6A, pp. 225–313.

[16] P. Kunze, “Apposition and superposition eyes,” in *Handbook of Sensory Physiology*, H. Autrum, Ed. Springer-Verlag, 1979, vol. VII/6A, pp. 442–502.

[17] K. Kirschfeld, “Die projektion der optischen umwelt auf das raster der rhabdomere im komplexauge von musca,” *Experimental Brain Research*, vol. 3, pp. 248–270, 1967.

[18] K. Kirschfeld, “The resolution of lens and compound eyes,” in *Neural Principles in Vision*, F. Zettler and R. Weiler, Eds. Springer Verlag, 1976, pp. 354–370.

[19] J. W. Duparre and F. C. Wippermann, “Micro-optical artificial compound eyes,” *IOP Journal of Bioinspiration & Biomimetics*, vol. 1, pp. R1–R16, 2006.

[20] N. Franceschini, J. M. Pichon, C. Blanes, and J. M. Brady, “From insect vision to robot vision,” *Phil. Trans. R. Soc. Lond. B: Biol. Sci.*, vol. 337, no. 1281, pp. 283–294, Sep. 1992.

[21] M. F. Land, “Visual acuity in insects,” *Annu. Rev. Entomol.*, vol. 42, pp. 147–177, 1997.

[22] W. S. Geisler, “Physical limits of acuity and hyperacuity,” *J. Opt. Soc. Am. A*, vol. 1, no. 7, pp. 775–782, Jul. 1984.

[23] M. Fahle and T. Poggio, “Visual hyperacuity: Spatiotemporal interpolation in human vision,” *Phil. Trans. R. Soc. Lond. B: Biol. Sci.*, vol. 213, no. 1193, pp. 451–477, Nov. 1981.

[24] G. Westheimer and S. P. McKee, “Spatial configurations for visual hyperacuity,” *Vision Research*, vol. 17, no. 8, pp. 941–947, 1977.

[25] G. Westheimer, “Diffraction theory and visual hyperacuity,” *Am. J. Optom. Physiol. Opt.*, vol. 53, no. 7, pp. 362–364, Jul. 1976.

[26] V. Braitenberg, “Patterns of projection in the visual system of the fly,” *Experimental Brain Research*, vol. 3, pp. 271–298, 1967.

[27] R. Hardie, “Functional organization of the fly retina,” in *Progress in Sensory Physiology*, D. Ottoson, Ed. Springer-Verlag, 1985, vol. V, pp. 1–79.

[28] C. Boschek, “On the fine structure of the peripheral retina and lamina ganglionaris of the fly, Musca domestica,” *Z. Zellforsch*, vol. 118, pp. 369–409, 1971.

[29] M. F. Land, “Optics and vision in invertebrates,” in *Handbook of Sensory Physiology*, H. Autrum, Ed. Springer-Verlag, 1981, vol. VII/6B, pp. 472–592.

[30] B. Pick, “Specific misalignments of rhabdomere visual axes in the neural superposition eye of dipteran flies,” *Biological Cybernetics*, vol. 26, pp. 215–224, 1977.

[31] R. S. Prabhakara, C. H. G. Wright, and S. F. Barrett, “Motion Detection: a Biomimetic Vision Sensor versus a CCD Camera Sensor,” *IEEE Sensors Journal*, vol. 12, no. 2, pp. 298–307, February 2012. (Invited paper). DOI: 10.1109/JSEN.2010.2100039

[32] G. P. Luke, C. H. G. Wright, and S. F. Barrett, “A Multi-Aperture Bio-Inspired Sensor with Hyperacuity,” *IEEE Sensors Journal*, vol. 12, no. 2, pp. 308–314, February 2012. (Invited paper). DOI: 10.1109/JSEN.2010.2099112

[33] M. R. Stephens, C. H. G. Wright, and S. F. Barrett, “Improved Motion Detection Method Using Spot Localization,” *ISA Biomedical Sciences Instrumentation*, vol. 47, pp. 171–176, Apr. 2011.

[34] J. A. Anderson, S. F. Barrett, and C. H. G. Wright, “Fly Eye Based Sensor Model and Animation Using MATLAB,” *ISA Biomedical Sciences Instrumentation*, vol. 47, pp. 300–304, Apr. 2011.

[35] B. K. Dean, C. H. G. Wright, and S. F. Barrett, “Preliminary Tests of a Possible Outdoor Light Adaptation Solution of a Fly Inspired Visual Sensor: A Biomimetic Solution,” *ISA Biomedical Sciences Instrumentation*, vol. 47, pp. 147–152, Apr. 2011.

[36] R. W. Streeter, S. F. Barrett, and C. H. G. Wright, “Signal Artifacts in a Light-Adapted, Musca domestica-based Sensor System,” *ISA Biomedical Sciences Instrumentation*, vol. 47, pp. 29–34, Apr. 2011.

[37] B. K. Dean, C. H. G. Wright, and S. F. Barrett, “Advances in Sensor Adaptation to Changes in Ambient Light: A Bio-inspired solution,” *ISA Biomedical Sciences Instrumentation*, vol. 46, pp. 20–25, Apr. 2010.

[38] R. W. Streeter, S. F. Barrett, and C. H. G. Wright, “Musca domestica Based Machine Vision Sensor: a Continuing Project,” *ISA Biomedical Sciences Instrumentation*, vol. 46, pp. 33–38, Apr. 2010.

[39] J. D. Davis, S. F. Barrett, C. H. G. Wright, and M. J. Wilcox, “Bio-Inspired Apposition Compound Eye Machine Vision Sensor System,” *IOP Journal of Bioinspiration & Biomimetics*, vol. 4, December 2009. Paper 046002.

[40] B. K. Dean, C. H. G. Wright, and S. F. Barrett, “The design of an analog module for sensor adaptation to changes in ambient light,” *ISA Biomedical Sciences Instrumentation*, vol. 45, pp. 185–190, Apr. 2009.
[41] G. P. Luke, C. H. G. Wright, and S. F. Barrett, “Software model of improved bio-inspired sensor,” *ISA Biomedical Sciences Instrumentation*, vol. 45, pp. 179–184, Apr. 2009.
[42] D. T. Riley, W. Harman, S. F. Barrett, and C. H. G. Wright, “Musca domestica Inspired Machine Vision Sensor with Hyperacuity,” *IOP Journal of Bioinspiration & Biomimetics*, vol. 3, no. 2, June 2008.
[43] J. B. Benson, C. H. G. Wright, and S. F. Barrett, “Redesign and Construction of an Artificial Compound Eye Visual Sensor,” *ISA Biomedical Sciences Instrumentation*, vol. 44, pp. 367–372, Apr. 2008.
[44] S. F. Barrett, J. B. Benson, and C. H. G. Wright, “Information Processing from a One-Dimensional Bio-Inspired Analog Sensor,” *ISA Biomedical Sciences Instrumentation*, vol. 44, pp. 63–68, Apr. 2008.
[45] J. D. Davis, S. F. Barrett, C. H. G. Wright, and M. J. Wilcox, “Bio-Inspired Minimal Machine Multi-Aperture Apposition Vision System,” *ISA Biomedical Sciences Instrumentation*, vol. 44, pp. 373–379, Apr. 2008.
[46] L. A. Benson, S. F. Barrett, and C. H. G. Wright, “Characterization of selected elementary motion detector cells to image primitives,” *ISA Biomedical Sciences Instrumentation*, vol. 44, pp. 410–416, Apr. 2008.

## LIST OF SYMBOLS, ABBREVIATIONS, AND ACRONYMS

| | |
|---|---|
| 1D | one-dimensional |
| 2D | two-dimensional |
| ADC | analog-to-digital converter |
| AGC | automatic gain control |
| CCD | charge-coupled device |
| CMOS | complementary metal oxide semiconductor |
| CPU | central processing unit |
| DAC | digital-to-analog converter |
| GUI | graphical user interface |
| OFA | optical fiber array |
| PdA | photodiode array |
| RC | resistive-capacitive |
| RL | resistive-inductive |